Advances in Applied Mathematics and Mechanics
Adv. Appl. Math. Mech., Vol. **5**, No. 3, pp. 337-350

DOI: 10.4208/aamm.12-m1264
June 2013

Matching Boundary Conditions for Scalar Waves in Body-Centered-Cubic Lattices

Ming Fang[1,2], Xianming Wang[3], Zhihui Li[1] and Shaoqiang Tang[2,*]

[1] *Hypervelocity Aerodynamics Institute, China Aerodynamics Research and Development Center, P.O. Box 211, Mianyang 621000, Sichuan, China*
[2] *HEDPS, CAPT and LTCS, College of Engineering, Peking University, Beijing 100871, China*
[3] *Center for Combustion Energy and Department of Thermal Engineering, Tsinghua University, Beijing 100084, China*

Received 2 May 2012; Accepted (in revised version) 18 December 2012

Available online 30 April 2013

Abstract. Matching boundary conditions (MBC's) are proposed to treat scalar waves in the body-centered-cubic lattices. By matching the dispersion relation, we construct MBC's for normal incidence and incidence with an angle α. Multiplication of MBC operators then leads to multi-directional absorbing boundary conditions. The effectiveness are illustrated by the reflection coefficient analysis and wave packet tests. In particular, the designed M1M1 treats the scalar waves in a satisfactory manner.

AMS subject classifications: 65Z05, 70-08

Key words: Body-centered-cubic (BCC) crystalline solids, dispersion relation, matching boundary condition, reflection coefficient, scalar waves.

1 Introduction

Atomic simulations play an increasingly important role in exploring fundamental issues of materials science and their applications to micro, nano and multiscale physics for emerging technologies [21]. In such simulations, artificial boundary treatment is one of the core techniques to avoid non-physical results due to spurious reflections [29]. Due to the discrete features and dispersion [13,30], artificial boundary conditions [2,6,10,14] developed for continuous wave propagation problems can not be adopted directly here.

*Corresponding author.
Email: fangm@pku.edu.cn (M. Fang), wangxianming06@mails.tsinghua.edu.cn (X. Wang), lizhihui@mail.tsinghua.edu.cn (Z. Li), maotang@pku.edu.cn (S. Tang)

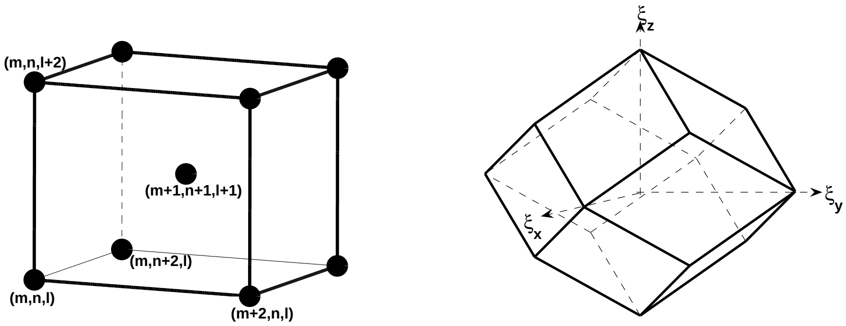

Figure 1: Unit cell (left) and first Brillouin zone (right) of BCC lattice.

Therefore effective absorbing boundary conditions are demanded to suppress effectively the reflections in atomic simulations.

In this paper, we consider a body-centered-cubic (BCC) lattice. As shown in Fig. 1, its unit cell has one lattice point in the center in addition to eight corner points. Many metals, such as Li, Na, K, Rb, W, Cs and Fe, take the BCC structure.

The simplest boundary condition for numerical simulations is the periodic boundary condition [4, 5, 7, 12, 16, 35]. As periodicity does not hold in most applications that require multiscale simulations, other boundary treatments have been developed for the BCC lattice. For instance, a flexible boundary condition was developed for simulating dislocations [25–27]. It is an iterative method using the superposition of Green's functions computed for plenty of atoms. Along this line, exact lattice Green's function may be computed for a semi-infinite lattice, leading to the time history kernel treatment and the bridging scale method [8, 15, 23, 24]. However, for the three dimensional BCC lattice, the calculation of the kernel functions is complicated, involving the inverse Laplace transforms and the Fourier transforms. Furthermore, the trade-off of the convolution cut-off time and the accuracy should be made according to specific applications. We also notice that a discrete boundary treatment was developed in terms of variational boundary conditions [17,18]. It considerably reduces the computing cost. Yet the design of such conditions requires to solve an optimization problem, which is time-step dependent and complicated for the three dimensional lattice.

As an alternative, matching boundary conditions (MBC's) were proposed recently [32–34]. Such conditions take the form of linear combinations of displacements and velocities at selected atoms near the artificial boundary. The combination coefficients are determined by matching the dispersion relation. MBC's perform very well in one-dimensional monoatomic chains, one-dimensional diatomic chains, two-dimensional square lattices and two-dimensional hexagonal lattices. Simplicity and essentially no additional computing load are the two major advantages for this class of boundary conditions.

In this paper, we extend the MBC's to treat scalar waves in the BCC lattice. By matching the dispersion relation, we construct MBC's for normal incidence and incidence with an angle α. Then by using the multiplication of MBC operators, we design multi-directional absorbing boundary conditions. The effectiveness of the designed MBC's are tested by reflection coefficient analysis and numerical examples similar to those in [34].

The rest of the paper is planned as follows. In Section 2, we design the MBC's for the BCC lattice. Then we demonstrate the effectiveness by the reflection coefficient analysis in Section 3 and numerical tests in Section 4. Some concluding remarks are made in Section 5.

2 Design of MBC's for BCC lattice

2.1 BCC lattice and its dispersion relation

In the BCC lattice, atoms occupy the staggered location (m,n,l) as illustrated in Fig. 1. Planes with a constant value m, n or l are coplanar with the crystallographic planes (1,0,0), (0,1,0) or (0,0,1), respectively. In this study, we investigate scalar waves under the harmonic potential, and account for the nearest neighboring interaction only.

Rescaled Newton's equation for an atom (m,n,l) reads

$$\begin{aligned}\ddot{u}_{m,n,l}=&u_{m+1,n+1,l+1}+u_{m-1,n-1,l-1}+u_{m-1,n+1,l+1}+u_{m+1,n-1,l-1}+u_{m+1,n-1,l+1}\\&+u_{m-1,n+1,l-1}+u_{m-1,n-1,l+1}+u_{m+1,n+1,l-1}-8u_{m,n,l}.\end{aligned}\tag{2.1}$$

Here $u_{m,n,l}(t)$ denotes the displacement. The purpose of studying the scalar waves is twofold. First, it lays a basis for the design of absorbing boundary conditions in realistic vector wave propagation. Secondly, it also serves as a discretization of the wave equation in a staggered grid, which has potential applications, e.g., in simulating the Navier-Stokes equations [1,31].

We seek for monochromatic wave solution

$$u_{m,n,l}=\exp\Big\{i\Big(\omega t+\frac{m}{2}\xi_x+\frac{n}{2}\xi_y+\frac{l}{2}\xi_z\Big)\Big\},\tag{2.2}$$

where ω is the frequency and (ξ_x,ξ_y,ξ_z) is the wave vector. The dispersion relation is readily obtained as follows

$$\omega(\xi_x,\xi_y,\xi_z)=2\sqrt{2-2\cos\frac{\xi_x}{2}\cos\frac{\xi_y}{2}\cos\frac{\xi_z}{2}}.\tag{2.3}$$

The first Brillouin zone is a rhombic dodecahedron [3], also shown in Fig. 1.

2.2 Unidirectional MBC's

Suppose that we simulate only half of the infinite lattice with $l\geq 0$. Boundary conditions are needed at the artificial boundary atoms with $l=0$. Similar to the one dimensional case, a general boundary condition can be formulated in the velocity-displacement form. Following the two dimensional lattice approach in [34] and considering the symmetry, we propose for each boundary atom $u_{m,n,0}$,

$$\begin{aligned}&\dot{u}_{m,n,0}+c_1(\dot{u}_{m+1,n+1,1}+\dot{u}_{m-1,n+1,1}+\dot{u}_{m+1,n-1,1}+\dot{u}_{m-1,n-1,1})\\=&b_0u_{m,n,0}+b_1(u_{m+1,n+1,1}+u_{m-1,n+1,1}+u_{m+1,n-1,1}+u_{m-1,n-1,1}).\end{aligned} \tag{2.4}$$

To facilitate later discussions, we introduce shift operators K_x,K_y and K_z defined by $K_xu_{m,n,l}=u_{m+1,n,l}$, $K_yu_{m,n,l}=u_{m,n+1,l}$ and $K_zu_{m,n,l}=u_{m,n,l+1}$. The boundary condition (2.4) can be rewritten as

$$\Big[Q(K_x,K_y,K_z)\frac{d}{dt}-P(K_x,K_y,K_z)\Big]u_{m,n,0}=0. \tag{2.5}$$

Here

$$\left\{\begin{aligned}Q(K_x,K_y,K_z)&=I+c_1(K_xK_y+K_x^{-1}K_y+K_xK_y^{-1}+K_x^{-1}K_y^{-1})K_z,\\P(K_x,K_y,K_z)&=b_0I+b_1(K_xK_y+K_x^{-1}K_y+K_xK_y^{-1}+K_x^{-1}K_y^{-1})K_z.\end{aligned}\right. \tag{2.6}$$

We define the matching residual function

$$\begin{aligned}\Delta(\xi_x,\xi_y,\xi_z)=&i\omega(\xi_x,\xi_y,\xi_z)\Big(1+4c_1e^{i\frac{\xi_z}{2}}\cos\frac{\xi_x}{2}\cos\frac{\xi_y}{2}\Big)\\&-\Big(b_0+4b_1e^{i\frac{\xi_z}{2}}\cos\frac{\xi_x}{2}\cos\frac{\xi_y}{2}\Big).\end{aligned} \tag{2.7}$$

Same as its one-dimensional counterpart, this function measures the quality of the boundary condition (2.4) for monochromatic wave with the wave vector (ξ_x,ξ_y,ξ_z). Perfect transmission is guaranteed at a wave vector when this function vanishes.

We first consider the normal incidence with $(\xi_x,\xi_y,\xi_z)=(0,0,\xi)$. The matching residual function reduces to

$$\Delta(0,0,\xi)=i\omega_{0,0}(\xi)\big(1+4c_1e^{i\frac{\xi}{2}}\big)-\big(b_0+4b_1e^{i\frac{\xi}{2}}\big). \tag{2.8}$$

Requiring $\Delta(0,0,\xi)=o(\xi^2)$, we calculate the coefficients c_1, b_0 and b_1, and obtain a boundary condition called as MBC1

$$\begin{aligned}&\dot{u}_{m,n,0}+\frac{1}{4}(\dot{u}_{m+1,n+1,1}+\dot{u}_{m-1,n+1,1}+\dot{u}_{m+1,n-1,1}+\dot{u}_{m-1,n-1,1})\\=&-4u_{m,n,0}+(u_{m+1,n+1,1}+u_{m-1,n+1,1}+u_{m+1,n-1,1}+u_{m-1,n-1,1}).\end{aligned} \tag{2.9}$$

For later comparative studies, we set $c_1=0$ and require $\Delta(0,0,\xi)=o(\xi)$. This leads to the velocity interfacial condition (VIC1) as follows [28].

$$\dot{u}_{m,n,0}=-2u_{m,n,0}+\frac{1}{2}(u_{m+1,n+1,1}+u_{m-1,n+1,1}+u_{m+1,n-1,1}+u_{m-1,n-1,1}). \tag{2.10}$$

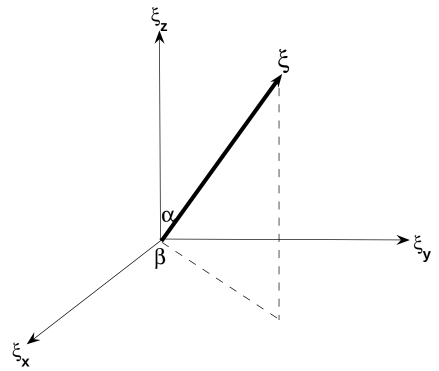

Figure 2: Wave vector with incident angle α and β.

To design boundary conditions for perfectly absorption of a scalar wave with incident angle α and β in the long wave limit, as shown in Fig. 2, for VIC1 we require $\Delta(\xi\sin\alpha\cos\beta,\xi\sin\alpha\sin\beta,\xi\cos\alpha)=o(\xi)$. This results in

$$\left[Q(K_x,K_y,K_z)\frac{d}{dt}-aP(K_x,K_y,K_z)\right]u_{m,n,0}=0, \tag{2.11}$$

where $a=1/\cos\alpha$ is the apparent wave propagation speed [20]. We name it as VIC1-a. Analogously, we adopt the concept of apparent wave propagation speed and choose the same form as (2.11) for MBC1-a. In this regard, the normal incidence boundary condition MBC1 is the same as MBC1-1, while VIC1 is the same as VIC1-1.

Atoms on an edge or at a corner may be treated in a similar way. For instance, at an atom $(m,0,0)$ on the edge, MBC1 reads

$$\dot{u}_{m,0,0}+\frac{1}{2}(\dot{u}_{m+1,1,1}+\dot{u}_{m-1,1,1})=-4u_{m,0,0}+2(u_{m+1,1,1}+u_{m-1,1,1}), \tag{2.12}$$

while VIC1 reads

$$\dot{u}_{m,0,0}=-2u_{m,0,0}+(u_{m+1,1,1}+u_{m-1,1,1}). \tag{2.13}$$

For the atom $(0,0,0)$ at the corner, MBC1 reads

$$\dot{u}_{0,0,0}+\dot{u}_{1,1,1}=-4u_{0,0,0}+4u_{1,1,1}, \tag{2.14}$$

while VIC1 reads

$$\dot{u}_{0,0,0}=-2u_{0,0,0}+2u_{1,1,1}. \tag{2.15}$$

2.3 Multi-directional MBC's

Following the pioneering work of Higdon [14] and experiences in [34], we use operator multiplication to treat general incidence. We take two apparent wave propagation speeds

a_1 and a_2. The operator multiplication

$$\Big[Q\frac{d}{dt}-a_1P\Big]\Big[Q\frac{d}{dt}-a_2P\Big]u_{m,n,0}=0 \tag{2.16}$$

yields a force boundary condition, named as V1V1(a_1,a_2) or M1M1(a_1,a_2), respectively, depending on the form of the chosen Q and P.

After some straightforward calculations, we obtain M1M1(a_1,a_2)

$$\begin{aligned}\ddot{u}_{m,n,0}=&-\frac{1}{2}(\ddot{u}_{m+1,n+1,1}+\ddot{u}_{m+1,n-1,1}+\ddot{u}_{m-1,n+1,1}+\ddot{u}_{m-1,n-1,1})\\&-\frac{1}{16}(\ddot{u}_{m+2,n+2,2}+\ddot{u}_{m+2,n-2,2}+\ddot{u}_{m-2,n+2,2}+\ddot{u}_{m-2,n-2,2})\\&-\frac{1}{8}(\ddot{u}_{m+2,n,2}+\ddot{u}_{m-2,n,2}+\ddot{u}_{m,n+2,2}+\ddot{u}_{m,n-2,2})-\frac{1}{4}\ddot{u}_{m,n,2}\\&+(a_1+a_2)\Big[-4\dot{u}_{m,n,0}+\frac{1}{4}(\dot{u}_{m+2,n+2,2}+\dot{u}_{m+2,n-2,2}+\dot{u}_{m-2,n+2,2}+\dot{u}_{m-2,n-2,2})\\&+\frac{1}{2}(\dot{u}_{m+2,n,2}+\dot{u}_{m-2,n,2}+\dot{u}_{m,n+2,2}+\dot{u}_{m,n-2,2})+\dot{u}_{m,n,2}\Big]\\&-a_1a_2\Big[16u_{m,n,0}-8(u_{m+1,n+1,1}+u_{m-1,n+1,1}+u_{m+1,n-1,1}+u_{m-1,n-1,1})\\&+(u_{m+2,n+2,2}+u_{m-2,n+2,2}+u_{m+2,n-2,2}+u_{m-2,n-2,2})\\&+2(u_{m,n+2,2}+u_{m,n-2,2}+u_{m+2,n,2}+u_{m-2,n,2})+4u_{m,n,2}\Big].\end{aligned} \tag{2.17}$$

Similarly, V1V1(a_1,a_2) reads

$$\begin{aligned}\ddot{u}_{m,n,0}=&(a_1+a_2)\Big[-2\dot{u}_{m,n,0}+\frac{1}{2}(\dot{u}_{m+1,n+1,1}+\dot{u}_{m-1,n+1,1}+\dot{u}_{m+1,n-1,1}+\dot{u}_{m-1,n-1,1})\Big]\\&-a_1a_2\Big[4u_{m,n,0}-2(u_{m+1,n+1,1}+u_{m-1,n+1,1}+u_{m+1,n-1,1}+u_{m-1,n-1,1})\\&+\frac{1}{4}(u_{m+2,n+2,2}+u_{m-2,n+2,2}+u_{m+2,n-2,2}+u_{m-2,n-2,2})\\&+\frac{1}{2}(u_{m,n+2,2}+u_{m,n-2,2}+u_{m+2,n,2}+u_{m-2,n,2})+u_{m,n,2}\Big].\end{aligned} \tag{2.18}$$

For an atom on the edge, M1M1(a_1,a_2) takes the form

$$\begin{aligned}\ddot{u}_{m,0,0}=&-\ddot{u}_{m+1,1,1}-\ddot{u}_{m-1,1,1}-\frac{1}{4}(\ddot{u}_{m+2,2,2}+\ddot{u}_{m-2,2,2}+2\ddot{u}_{m,2,2})\\&+(a_1+a_2)\big[-4\dot{u}_{m,0,0}+(\dot{u}_{m+2,2,2}+\dot{u}_{m-2,2,2}+2\dot{u}_{m,2,2})\big]\\&-a_1a_2\big[16u_{m,0,0}-16(u_{m+1,1,1}+u_{m-1,1,1})+4(u_{m+2,2,2}+u_{m-2,2,2}+2u_{m,2,2})\big],\end{aligned} \tag{2.19}$$

while V1V1(a_1,a_2) reads

$$\begin{aligned}\ddot{u}_{m,0,0}=&(a_1+a_2)\big[-2\dot{u}_{m,0,0}+(\dot{u}_{m+1,1,1}+\dot{u}_{m-1,1,1})\big]\\&-a_1a_2\big[4u_{m,0,0}-4(u_{m+1,1,1}+u_{m-1,1,1})+(u_{m+2,2,2}+u_{m-2,2,2}+2u_{m,2,2})\big].\end{aligned} \tag{2.20}$$

For an atom at the corner, $\mathrm{M1M1}(a_1,a_2)$ reads

$$\begin{aligned}&\ddot{u}_{0,0,0}+2\ddot{u}_{1,1,1}+\ddot{u}_{2,2,2}\\ =&(a_1+a_2)[-4\dot{u}_{0,0,0}+4\dot{u}_{2,2,2}]-a_1a_2[16u_{0,0,0}-32u_{1,1,1}+16u_{2,2,2}],\end{aligned} \tag{2.21}$$

while $\mathrm{V1V1}(a_1,a_2)$ reads

$$\ddot{u}_{0,0,0}=(a_1+a_2)[-2\dot{u}_{0,0,0}+2\dot{u}_{1,1,1}]-a_1a_2[4u_{0,0,0}-8u_{1,1,1}+4u_{2,2,2}]. \tag{2.22}$$

3 Effectiveness of MBC's: reflection coefficient analysis

In [9, 11, 19, 32, 34], the reflection coefficients were calculated to check the effectiveness of the corresponding artificial boundary conditions for semi-infinite lattices. For a wave vector (ξ_x,ξ_y,ξ_z), we consider a downward harmonic wave

$$\begin{aligned}u_{m,n,l}(t)=&\exp\Big\{i\Big[\omega(\xi_x,\xi_y,\xi_z)t+\frac{m}{2}\xi_x+\frac{n}{2}\xi_y+\frac{l}{2}\xi_z\Big]\Big\}\\ &+\tilde{R}\exp\Big\{i\Big[\omega(\xi_x,\xi_y,-\xi_z)t+\frac{m}{2}\xi_x+\frac{n}{2}\xi_y-\frac{l}{2}\xi_z\Big]\Big\}.\end{aligned} \tag{3.1}$$

In the literature, $\tilde{R}$ denotes the amplitude of the reflected wave. Its modulus $|\tilde{R}|$ is usually called as the reflection coefficient. For the three dimensional BCC lattice, the situation is more complex. Noticing that the group velocity

$$v_g=\Big(\frac{\partial\omega}{\partial\xi_x},\frac{\partial\omega}{\partial\xi_y},\frac{\partial\omega}{\partial\xi_z}\Big) \tag{3.2}$$

identifies the propagation speed of a wave envelope, we observe that $\tilde{R}$ represents the reflection only when v_g points inward the atomic domain, i.e., $\partial\omega/\partial\xi_z>0$. If v_g points outward ($\partial\omega/\partial\xi_z<0$), then it is $1/\tilde{R}$ that represents the reflection.

After some calculations, we define the reflection coefficient as follows.

$$|R|=\begin{cases}\Big|\dfrac{\Delta(\xi_x,\xi_y,\xi_z)}{\Delta(\xi_x,\xi_y,-\xi_z)}\Big|, & \text{if } \dfrac{\partial\omega}{\partial\xi_z}\geq 0,\\ \Big|\dfrac{\Delta(\xi_x,\xi_y,-\xi_z)}{\Delta(\xi_x,\xi_y,\xi_z)}\Big|, & \text{if } \dfrac{\partial\omega}{\partial\xi_z}<0.\end{cases} \tag{3.3}$$

Two characteristic incident angles in the BCC lattice are 0 (normal incidence) and $\arcsin(\sqrt{3}/3)$. The latter corresponds to incidence along the diagonal of the unit cell. Therefore we consider the corresponding boundary conditions with $a=1$ and $a=\sqrt{3}$, respectively. Numerical test shows that, for either of MBC1, VIC1, MBC1-$\sqrt{3}$ and VIC1-$\sqrt{3}$, $|R|$ is not bigger than 1 in the positive half of the first Brillouin zone ($\xi_z>0$). This justifies that all of them may serve as absorbing boundary conditions. We illustrate the reflection coefficients in some planes within the first Brillouin zone. Fig. 3 gives the reflection

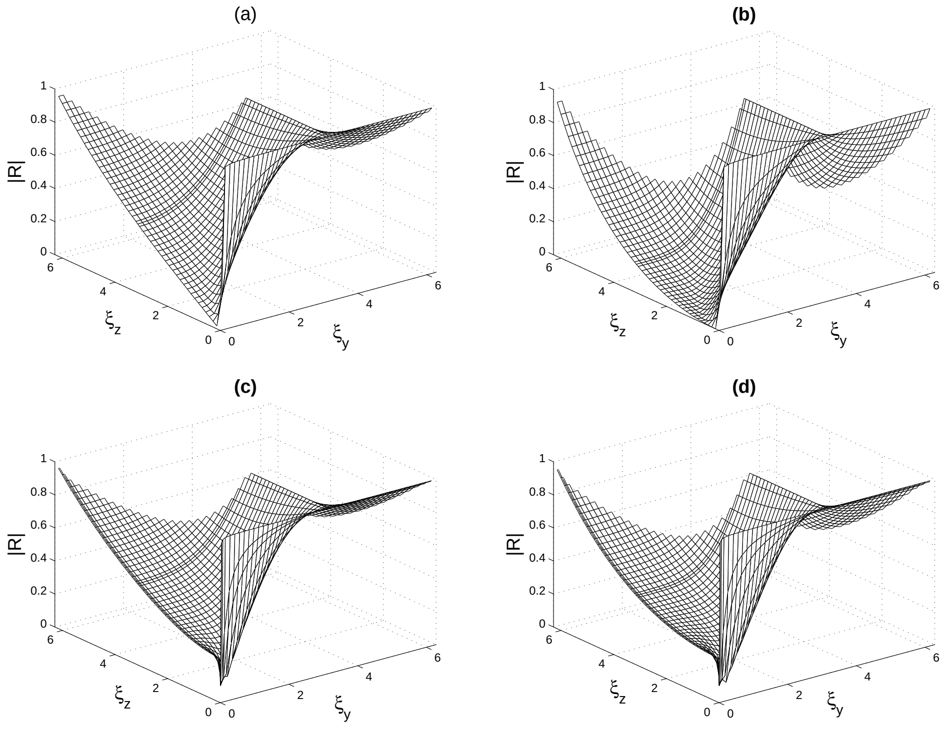

Figure 3: Reflection coefficient in the plane $\xi_x=0$: (a) VIC1, (b) MBC1, (c) VIC1-$\sqrt{3}$, (d) MBC1-$\sqrt{3}$.

coefficients in the plane $\xi_x=0$. For simplicity and clarity, we only plot a quarter of the plane. We observe that MBC's have better absorbing effect than VIC's, as seen from comparisons between (a) and (b), as well as (c) and (d). Fig. 4 gives the reflection coefficients in the plane $\xi_z=\pi$, also a quarter of the plane. Again we observe that MBC's have better absorbing effect than VIC's.

For multi-directional MBC's (2.17), we may prove that the reflection coefficient is

$$|R|=|R_1||R_2|, \tag{3.4}$$

where $|R_j|$ is reflection coefficient of the unidirectional MBC with a_j. As an example, Fig. 5 gives the reflection coefficient for M1M1(1,$\sqrt{3}$) and V1V1(1,$\sqrt{3}$) on the plane $\xi_z=\pi$. It is clear that the multiplication reduces reflection, and M1M1(1,$\sqrt{3}$) has better absorbing effect than V1V1(1,$\sqrt{3}$).

4 Numerical examples: wave packet tests

We perform atomic simulations with $40\times40\times40$ cells ($-40\le m,n,l\le 40$). Four kinds of boundary conditions are used, namely, VIC1, MBC1, V1V1(1,$\sqrt{3}$) and M1M1(1,$\sqrt{3}$).

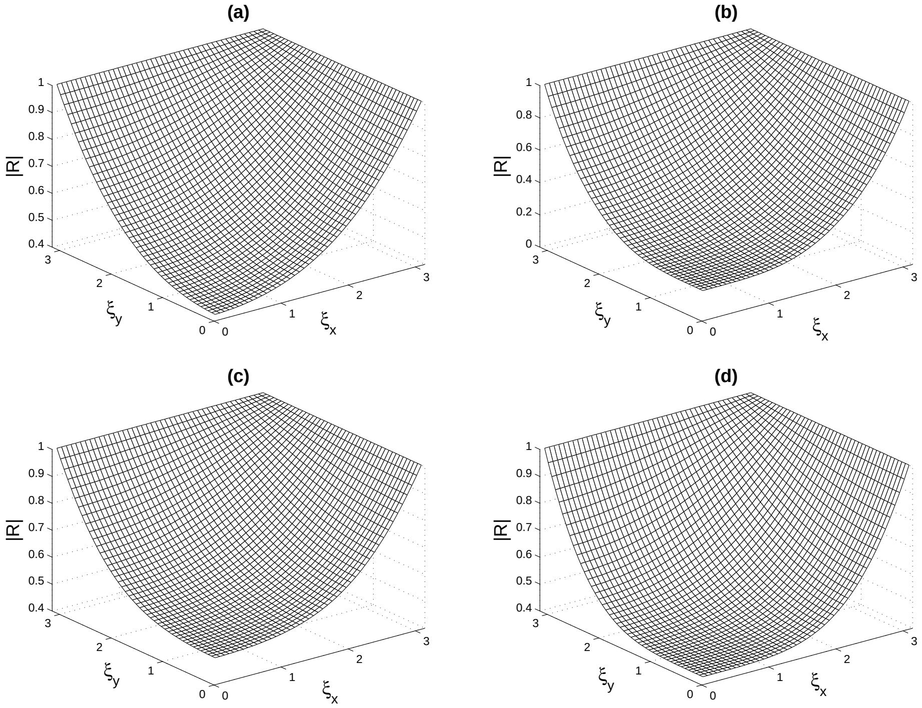

Figure 4: Reflection coefficient in the plane $\xi_z = \pi$: (a) VIC1, (b) MBC1, (c) VIC1-$\sqrt{3}$, (d) MBC1-$\sqrt{3}$.

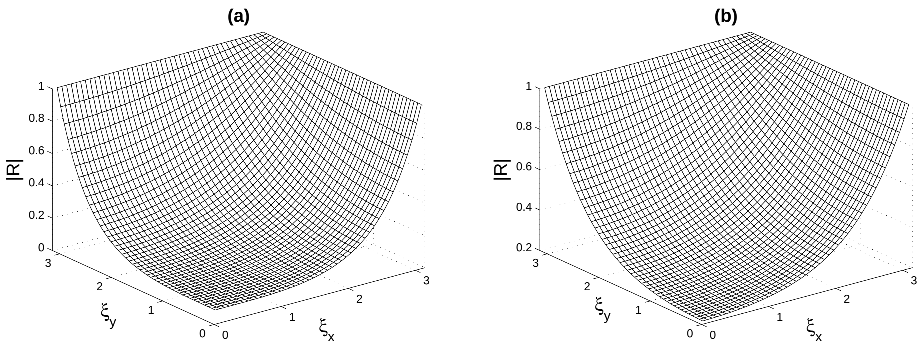

Figure 5: Reflection coefficient in the plane $\xi_z = \pi$: (a) M1M1$(1,\sqrt{3})$, (b) V1V1$(1,\sqrt{3})$.

For time integration of Newton's law, we use a speed Verlet scheme

$$\left\{\begin{aligned} u^{j+1}_{m,n,l} &= u^{j}_{m,n,l} + \dot{u}^{j}_{m,n,l}\Delta t + f^{j}_{m,n,l}\frac{\Delta t^2}{2}, \\ \dot{u}^{j+1}_{m,n,l} &= \dot{u}^{j}_{m,n,l} + \frac{\Delta t}{2}\big(f^{j}_{m,n,l} + f^{j+1}_{m,n,l}\big), \end{aligned}\right. \tag{4.1}$$

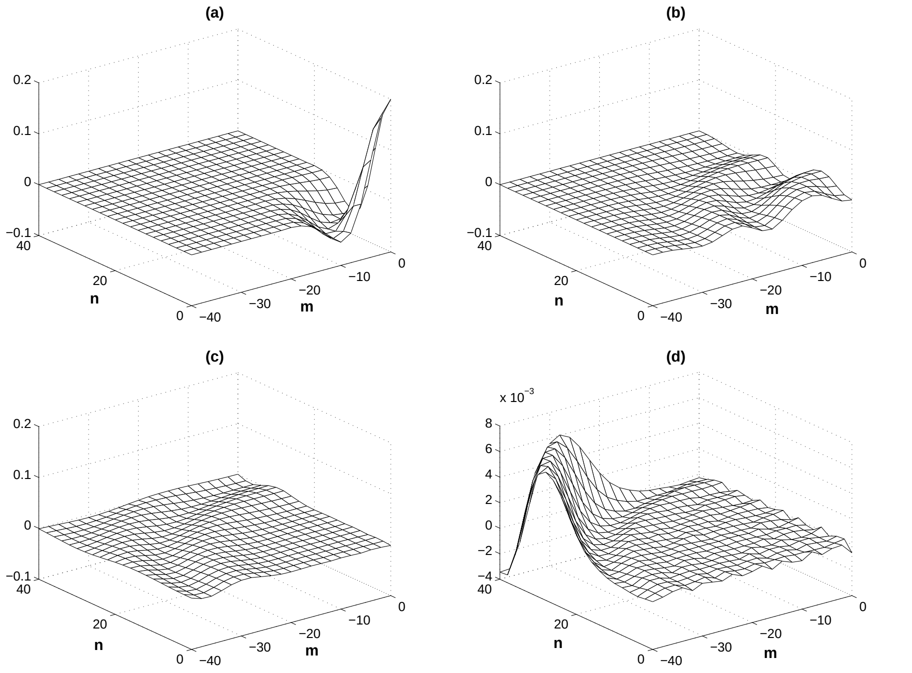

Figure 6: Wave propagation on the plane $l=0$: (a) $t=0$; (b) $t=10$; (c) $t=20$; (d) $t=30$.

with $\Delta t=1/64$. We take the following initial condition

$$u_{m,n,l}(0)=\begin{cases} e^{-r^2/25}\left(\cos\left(r\left(0.5+\dfrac{\pi}{40}\right)\right)+\cos\left(r\left(0.5-\dfrac{\pi}{40}\right)\right)\right), & |r|\le 10, \\ 0, & |r|>10, \end{cases} \tag{4.2a}$$

$$\dot{u}_{m,n,l}(0)=0, \tag{4.2b}$$

where $r^2=(m/2)^2+(n/2)^2+(l/2)^2$. This is a sinusoidal wave enveloped by an exponential function.

To make comparison, exact solutions are computed from simulations over a much larger domain. The evolution of the wave packet is illustrated on the central plane $l=0$ in Fig. 6. Due to symmetry, we just present a quarter of the plane. The initial wave propagates outward, reaching the boundary at about $t=20$. At $t=30$, the major part of the wave, except near the corner, has passed through the surface.

Fig. 7 shows the wave profiles at $t=30$ using various boundary conditions. All four boundary conditions provide reasonably good suppression of reflection. MBC's perform better than VIC's. M1M1($1,\sqrt{3}$) gives the best performance, indiscernible from the exact solution in Fig. 6(d).

To better illustrate the reflection suppression, we concentrate on the motion of the atom (38,0,0) near the mid-point of the boundary, and the atom (38,38,0) near the corner.

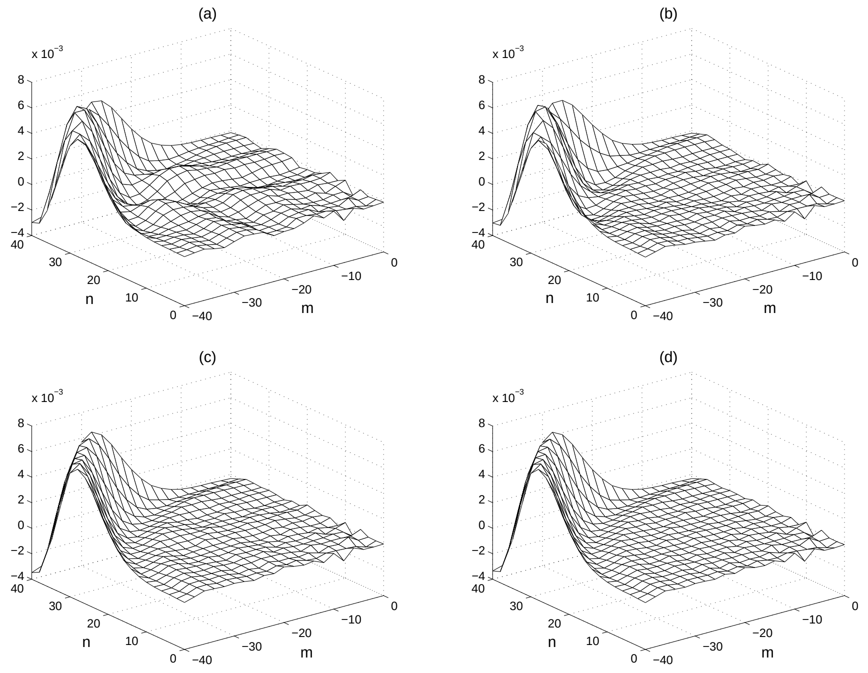

Figure 7: Wave profile on the plane $l=0$ at $t=30$: (a) VIC1, (b) MBC1, (c) V1V1$(1,\sqrt{3})$, (d) M1M1$(1,\sqrt{3})$.

For comparison, we plot the results of VIC1, MBC1 and the exact solution. For the atom (38,0,0), the main part of the wave has passed through the boundary from $t=30$ on. The reflections with MBC1 and VIC1 are not very big, and MBC1 has better absorbing effect. For the atom (38,38,0), specific treatments are desirable for the corner effect [22]. Nevertheless, these two boundary conditions can absorb the incident wave reasonably well.

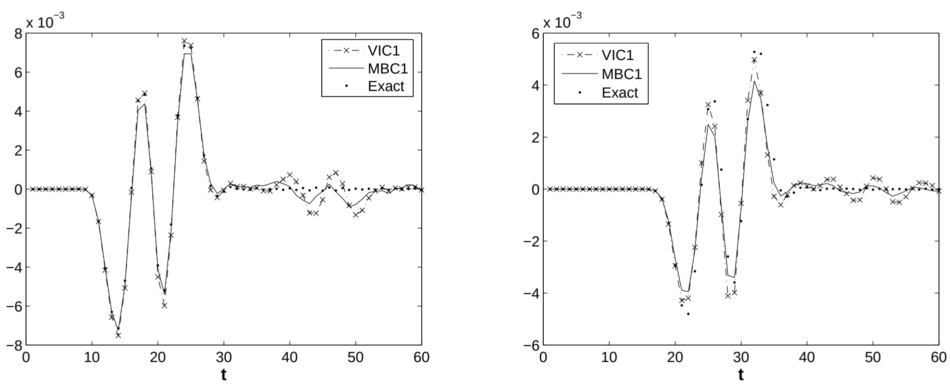

Figure 8: Displacements of specific atoms: (a) $u_{38,0,0}$, (b) $u_{38,38,0}$.

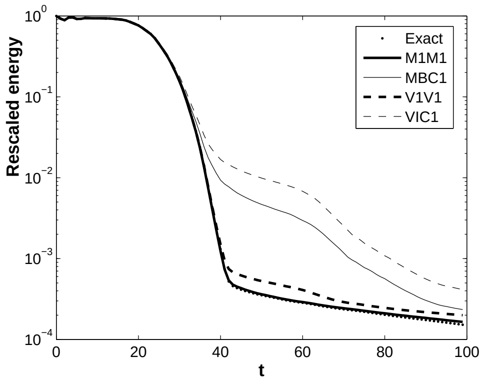

Figure 9: Total energy for wave packet test with $\xi_0 = 0.5$.

We define the total energy as follows.

$$E = \frac{1}{2}\sum_{inner} \dot{u}^2 + \sum_{i,j,k=odd} V(i,j,k), \tag{4.3}$$

where

$$V(i,j,k) = \frac{1}{2}\sum_{|m-i|=1}\sum_{|n-j|=1}\sum_{|l-k|=1} (u_{m,n,l} - u_{i,j,k})^2. \tag{4.4}$$

It quantifies the reflection suppression. In Fig. 9, we plot the energy rescaled by the initial value $E_0 = E(0)$. We observe again that MBC's have better absorbing effect than VIC's.

In summary, for wave profiles and total energy, MBC's perform better than VIC's. The MBC's, especially M1M1$(1,\sqrt{3})$, handle scalar waves in a satisfactory manner.

5 Conclusions

In this paper, we have developed matching boundary conditions for scalar waves in the three dimensional body-centered-cubic (BCC) lattice. The designed MBC's take a form of linear combination of displacements and velocities for selected atoms near the boundary. By matching the dispersion relation, we have designed MBC's perfectly absorbing normal incidence in the long wave limit, and derived the unidirectional MBC's with an incident angle α. Furthermore, the multi-directional MBC's have been obtained by using the products of MBC operators. For the designed MBC's, the reflection coefficient is not bigger than 1 in the positive half of the first Brillouin zone ($\xi_z > 0$). Numerical tests have demonstrated the effectiveness. MBC's perform better than VIC's. The designed M1M1 turns out to be efficient in suppressing numerical reflections.

Acknowledgments

This research is partially supported by NSFC under grant number 91016027 and National Basic Research Program of China under contract numbers 2010CB731500.

References

[1] S. W. ARMFIELD, *Finite difference solutions of the Navier-Stokes equations on staggered and non-staggered grids*, Comput. Fluids, 20 (1991), pp. 1–17.

[2] J. P. BERENGER, *A perfectly matched layer for the absorption of the electromagnetic waves*, J. Comput. Phys., 114 (1994), pp. 185–200.

[3] M. BORN AND K. HUANG, Dynamical Theory of Crystal Lattices, Clarendon Press, Oxford, 1954.

[4] C. BOS, J. SIETSMA AND B. J. THIJSSE, *Molecular dynamics simulation of interface dynamics during the fcc-bcc transformation of a martensitic nature*, Phys. Rev. B, 73 (2006), 104117.

[5] L. CHEN, C. WANG AND T. YU, *Molecular dynamics simulation of kink in $\langle 100 \rangle$ edge dislocation in body centered cubic iron*, Chin. Sci. Bull., 52 (2007), pp. 2291–2296.

[6] R. CLAYTON AND B. ENGQUIST, *Absorbing boundary condtions for acoustic and elastic wave equations*, Bull. Seism. Soc. Am., 67 (1977), pp. 1529–1540.

[7] A. M. CUITINO, L. STAINIER, G. WANG, A. STRACHAN, T. CAGIN, W. A. GODDARD AND M. ORTIZ, *A multiscale approach for moldeling crystalline solids*, J. Comput. Aided Mater., 8 (2002), pp. 127–149.

[8] M. DREHER AND S. TANG, *Time history interfacial conditions in multiscale computations of lattice oscillations*, Comput. Mech., 41 (2008), pp. 683–698.

[9] W. E AND Z. HUANG, *Matching conditions in atomistic-continuum modeling of materials*, Phys. Rev. Lett., 87 (2001), 135501.

[10] B. ENGQUIST AND A. MAJDA, *Radiation boundary conditions for acoustic and elastic calculations*, Comm. Pure Appl. Math., 32 (1979), pp. 313–357.

[11] M. FANG AND S. TANG, *Efficient and robust design for absorbing boundary conditions in atomistic computations*, Chin. Phys. Lett., 26 (2009), 116201.

[12] J. FIKAR AND R. SCHAUBLIN, *Molecular dynamics simulation of radiation damage in bcc tungsten*, J. Nuc. Mater., 386-388 (2009), pp. 97–101.

[13] M. N. GUDDATI AND S. THIRUNAVUKKARASU, *Phonon absorbing boundary conditions for molecular dynamics*, J. Comput. Phys., 228 (2009), pp. 8112–8134.

[14] R. L. HIGDON, *Absorbing boundary conditions for the wave equation*, Math. Comput., 49 (1987), pp. 65–90.

[15] E. G. KARPOV, H. YU, H. S. PARK, W. K. LIU, Q. J. WANG AND D. QIAN, *Multiscale boundary conditions in crystalline solids: theory and application to nanoindentation*, Int. J. Solids Struct., 43 (2006), pp. 6359–6379.

[16] S. A. KOTRECHKO, A. V. FILATOV AND A. V. OVSJANNIKOV, *Molecular dynamics simulation of deformation and failure of nanocrystals of bcc metals*, Theo. Appl. Frac. Mech., 45 (2006), pp. 92–99.

[17] X. LI AND W. E, *Multiscale modeling of the dynamics of solids at finite temperature*, J. Mech. Phys. Solids, 53 (2005), pp. 1650–1685.

[18] X. LI AND W. E, *Variational boundary conditions for molecular dynamics simulation of solids at low temperature*, Comm. Comput. Phys., 1 (2006), pp. 135–175.

[19] X. LI AND W. E, *Variational boundary conditions for molecular dynamics simulations of crystalline solids at finite temperature: treatment of the thermal bath*, Phys. Rev. B, 76 (2007), 104107.

[20] E. L. LINDMAN, *"Free-space" boundary conditions for the time dependent wave equation*, J. Comput. Phys., 18 (1975), pp. 66–78.

[21] W. K. LIU, E. G. KARPOV AND H. S. PARK, Nano Mechanics and Materials: Theory, Multiscale Methods and Applications, Wiley, New York, 2006.

[22] G. PANG AND S. TANG, *Time history kernel functions for square lattice*, Comput. Mech., 48 (2011), pp. 699–711.

[23] H. S. PARK, E. G. KARPOV, P. A. KLEIN AND W. K. LIU, *Three-dimensional bridging scale analysis of dynamic fracture*, J. Comput. Phys., 207 (2005), pp. 588–609.

[24] H. S. PARK, E. G. KARPOV AND W. K. LIU, *Non-reflecting boundary conditions for atomistic, continuum and coupled atomistic/continuum simulations*, Int. J. Numer. Methods Eng., 64 (2005), pp. 237–259.

[25] S. RAO, C. HERNANDEZ, J. P. SIMMONS, T. A. PARTHASARATHY AND C. WOODWARD, *Green's function boundary conditions in two-dimensional and three-dimensional atomistic simulations of dislocations*, Philos. Mag. A, 77 (1998), pp. 231–256.

[26] J. E. SINCLAIR, *Improved atomistic model of a bcc dislocation core*, J. Appl. Phys., 42 (1971), pp. 5321–5329.

[27] J. E. SINCLAIR, P. C. GEHLEN, R. G. HOAGLAND AND J. P. HIRTH, *Flexible boundary conditions and nonlinear geometric effects in atomic dislocation modeling*, J. Appl. Phys., 49 (1978), pp. 3890–3897.

[28] S. TANG, *A finite difference approach with velocity interfacial conditions for multiscale computations of crystalline solids*, J. Comput. Phys., 227 (2008), pp. 4038–4062.

[29] S. TANG AND M. FANG, *Unstable surface modes in finite chain computations: deficiency of reflection coefficient approach*, Commun. Comput. Phys., 8 (2010), pp. 143–158.

[30] A. C. TO AND S. LI, *Perfectly matched multiscale simulations*, Phys. Rev. B, 72 (2005), 035414.

[31] R. VERZICCO AND P. ORLANDI, *A finite-difference scheme for three-dimensional incompressible flows in cylindrical coordinates*, J. Comput. Phys., 123 (1996), pp. 402–414.

[32] X. WANG AND S. TANG, *Matching boundary conditions for diatomic chains*, Comput. Mech., 46 (2010), pp. 813–826.

[33] X. WANG, Matching Boundary Conditions for Atomic Simulations of Crystalline Solids, PhD thesis, Tsinghua University, Beijing, 2011.

[34] X. WANG AND S. TANG, *Matching boundary conditions for lattice dynamics*, Int. J. Numer. Methods Eng., 93 (2013), pp. 1255–1285.

[35] D. S. XU, R. YANG, J. LI, J. P. CHANG, H. WANG, D. LI AND S. YIP, *Atomistic simulation of the influence of pressure on dislocation between nucleation in bcc Mo*, Comput. Mater. Sci., 36 (2006), pp. 60–64.